CSF Flow Quantification of the Cerebral Aqueduct in Normal Volunteers Using Phase Contrast Cine MR Imaging

Jeong Hyun Lee, MD[1]
Ho Kyu Lee, MD[1]
Jae Kyun Kim, MD[1]
Hyun Jeong Kim, MD[1]
Ji Kang Park, MD[2]
Choong Gon Choi, MD[1]

Objective: To evaluate whether the results of cerebrospinal fluid (CSF) flow quantification differ according to the anatomical location of the cerebral aqueduct that is used and the background baseline region that is selected.

Materials and Methods: The CSF hydrodynamics of eleven healthy volunteers (mean age = 29.6 years) were investigated on a 1.5T MRI system. Velocity maps were acquired perpendicular to the cerebral aqueduct at three different anatomical levels: the inlet, ampulla and pars posterior. The pulse sequence was a prospectively triggered cardiac-gated flow compensated gradient-echo technique. Region-of-interest (ROI) analysis was performed for the CSF hydrodynamics, including the peak systolic velocity and mean flow on the phase images. The selection of the background baseline regions was done based on measurements made in two different areas, namely the anterior midbrain and temporal lobe, for 10 subjects.

Results: The mean peak systolic velocities showed a tendency to increase from the superior to the inferior aqueduct, irrespective of the background baseline region, with the range being from 3.30 cm/sec to 4.08 cm/sec. However, these differences were not statistically significant. In the case of the mean flow, the highest mean value was observed at the mid-portion of the ampulla (0.03 cm^3/sec) in conjunction with the baseline ROI at the anterior midbrain. However, no other differences were observed among the mean flows according to the location of the cerebral aqueduct or the baseline ROI.

Conclusion: We obtained a set of reference data of the CSF peak velocity and mean flow through the cerebral aqueduct in young healthy volunteers. Although the peak systolic velocity and mean flow of the CSF differed somewhat according to the level of the cerebral aqueduct at which the measurement was made, this difference was not statistically significant.

Index terms:
Cerebrospinal fluid, MR studies
Cerebrospinal fluid, flow dynamics
Cerebrospinal fluid, cine study

Korean J Radiol 2004;5:81-86
Received November 13, 2003; accepted after revision April 1, 2004.

Department of [1]Radiology, Asan Medical Center, Ulsan University College of Medicine; Department of [2]Radiology, Ulsan University Hospital, Ulsan University College of Medicine

This paper was presented in the form of a scientific poster at the 10th Scientific Meeting and Exhibition of ISMRM (2002).

Address reprint requests to:
Ho Kyu Lee, MD, Department of Radiology, Asan Medical Center, Ulsan University College of Medicine, 388-1 Poongnap-2dong, Songpa-gu, Seoul 138-736, Korea.
Tel. (822) 3010-4400
Fax. (822) 476-4719
e-mail: hklee2@amc.seoul.kr

Cardiac cycle-related cerebral blood volume variations produce bi-directional oscillatory movement of cerebrospinal fluid (CSF) within the craniospinal axis (1–7). During systole, the net inflow of blood increases the intracranial volume and induces craniocaudal (systolic) CSF flow. During diastole, the net outflow of blood decreases the intracranial volume and promotes caudocranial (diastolic) CSF flow. Phase-contrast magnetic resonance (MR) imaging can display this pulsatory CSF motion non-invasively and allows the assessment of its amplitude (2–7). This technique sensitizes MR images to velocity changes in a specific direction, while cancelling signals from stationary protons and from motion in other directions (8). Hydrocephalus is caused by a disturbance of the CSF hydrodynamics. Pathological CSF flow dynamics in the obstructive and non-obstructive hydrocephalus have been

extensively analyzed using phase-contrast MR imaging (2, 8−15). Elevated CSF flow through the cerebral aqueduct has also been reported in patients with normal pressure hydrocephalus who subsequently responded to ventriculoperitoneal shunting (9−11, 13). Nevertheless, the clinical utility of CSF flow velocity analysis has remained limited, due to the wide variation of the CSF flow values observed in normal subjects (6, 16−18).

Anatomically, the cerebral aqueduct is divided into three parts, namely the pars anterior, ampulla and pars posterior, which are separated by two natural constrictions of the aqueductal lumen, one in the middle of the superior colliculus and the other at the level of the intercollicular sulcus (Fig. 1A). The pars posterior has the narrowest lumen of the cerebral aqueduct, while the ampulla has the widest lumen (19). Previous studies of CSF flow dynamics were made at a variety of different locations of the cerebral aqueduct, such as the mid-portion, the level of the inferior colliculi, or the junction with the fourth ventricle (18, 20, 21). To the best of our knowledge, however, there has been no study on the effects of scan level on CSF flow quantification.

One thing that must be considered for CSF flow analysis using 2D cine phase-contrast MR imaging is the possible residual systematic errors caused by imperfect suppression of eddy currents or brain motion. Therefore, to correct these possible residual systematic errors, a background baseline region representing the apparent velocity in a region of no flow must be recorded and subtracted from the apparent velocities in the ROI. However, so far as we know, there has been no study on the effects of the background baseline region on CSF flow quantification either.

The purpose of this study was to evaluate whether the results of CSF flow quantification obtained using two-dimensional cine phase contrast MR imaging differ according to the anatomical location of the aqueduct at which the measurements are taken in healthy volunteers. We also evaluated the effect of the background baseline region on the results of the CSF flow quantification in several different locations.

MATERIALS AND METHODS

Eleven healthy volunteers (2 men and 9 women; age range, 27−31 years; mean age, 29.3 years), who were free from neurologic disease, had no cerebrovascular risk factors and had no history of medication, were enrolled in this study. They were examined on a 1.5 Tesla whole-body scanner (Magnetom Vision; Siemens, Erlangen, Germany) using a standard head coil; the head was not tilted in any specific way. The aqueduct was visualized using a sagittal T2-weighted fast spin echo technique (4000 msec/99 msec/2 [TR/TE/excitations]). In all volunteers, velocity maps were acquired in an oblique axial plane perpendicular to the aqueduct at three different anatomical levels, namely the inlet, the ampulla and the pars posterior (Fig. 1B). A cardiac-gated flow compensated gradient echo

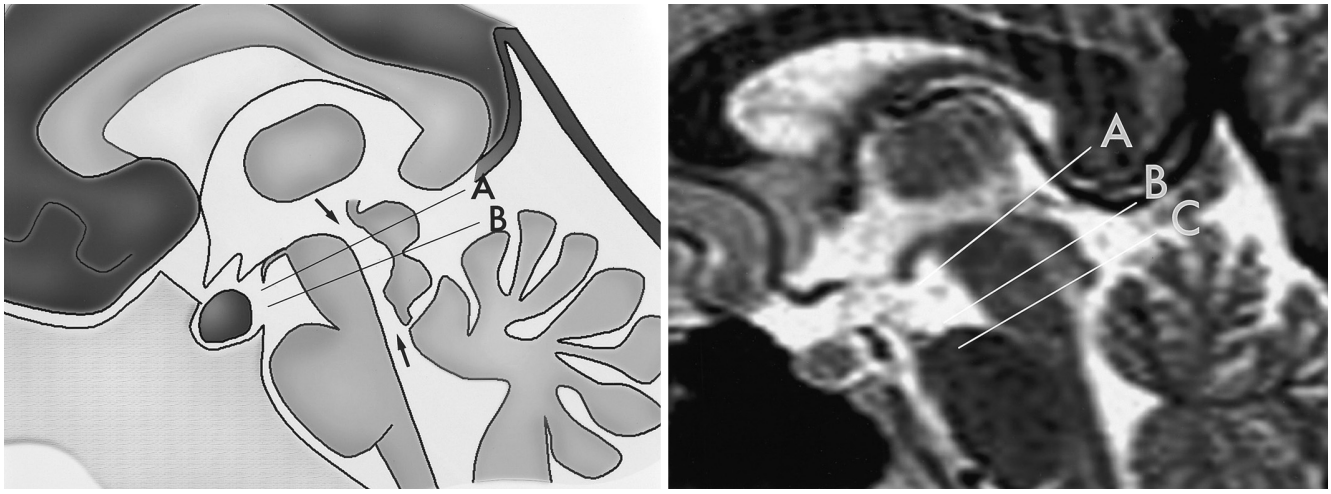

A B

Fig. 1. A. Normal anatomy of the cerebral aqueduct as viewed in the sagittal plane. The two arrows indicate the proximal and the distal ends of the cerebral aqueduct. The solid lines indicated by an A (the middle of the superior colliculus) and by a B (the level of the intercollicular sulcus) divide the aqueduct into the pars anterior, ampulla and pars posterior, craniocaudally, with the ampulla having the widest diameter and the pars posterior having the narrowest diameter.
B. Midline sagittal T2-weighted image showing the positions of the localizers for the velocity map at each level of the cerebral aqueduct. The solid lines indicate the different positions of the localizers of the oblique axial images set perpendicular to the aqueduct of Sylvius. A; the inlet, B; the ampulla, C; the pars posterior.

sequence with flow velocity encoding of 10 cm/sec in the slice-selective direction was used with the following parameters: 45 msec/12 msec/1 (TR/TE/excitations), 10° flip angle, 14 ×20 cm field of view, 256 ×512 matrix, and 4 mm slice thickness. The in-plane spatial resolution was 0.54 mm ×0.39 mm ×4 mm. The sequence was prospectively triggered by every heartbeat with a delay of 20 msec applied to the first frame. Cardiac gating produced a series of magnitude and phase-contrast images at different cardiac phases (8−15 phases).

Phase-contrast images were displayed on a gray scale, where high signal intensity indicated caudal flow and low intensity represented rostral flow. CSF flow quantification was performed on those phase images showing maximum velocity, using the region-of-interest (ROI) measurements. The ROI measurement was performed by one of the authors at the independent console in all cases, until the optimum CSF velocity curve was obtained. A circular ROI was drawn so to include those pixels that reflected the CSF flow signals of the cerebral aqueduct on the phase images with maximum flow rates. The mean area of the circular ROI was 2.8 mm^2 (range, 2−5 mm^2). To correct the possible residual systematic errors caused by imperfect suppression of eddy currents or brain motion, a background baseline value representing the apparent velocity in a region of no flow was recorded and subtracted from the apparent velocities in the ROI. The background baseline values were obtained at two different locations in 10 of the 11 subjects, one at the midbrain anterior to the aqueduct and the other at a point just lateral to the left temporal lobe (Fig. 2). Following the acquisition of the CSF flow velocity curves in all cases, the CSF hydrodynamics were analyzed in terms of the peak systolic velocity and mean flow. The mean flow was calculated from the following equation: mean flow (cm^3/sec) = mean velocity (cm/sec) x area of ROI (cm^2), where the mean velocity was automatically determined from the mean value of the measured velocities of each cardiac phase. A circular ROI drawn for those pixels reflecting the CSF flow signal was substituted for the diameter of the aqueduct, because the phase images did not show the real anatomical lumen of the aqueduct, but only the CSF flow.

We evaluated whether the results of the CSF flow quantification differed according to the anatomical location and/or the background baseline region. The statistical analysis was performed using the SPSS/PC™ statistical package. The Kruskal-Wallis test was used to compare the values obtained at the three different locations of the aqueduct between the two background baseline regions. Null hypotheses were verified using a 2-sided test and *p*-values smaller than 0.05 were considered significant.

RESULTS

In all of the subjects, a typical sinusoidal pattern of CSF flow was observed during the cardiac cycle. Table 1 shows the mean peak systolic velocities and mean flows of the cerebral aqueduct according to the three different locations and the two different baseline regions. The mean peak systolic velocities showed a tendency to increase from the superior to the inferior aqueduct, irrespective of the background baseline region. The values obtained with the baseline region at the anterior midbrain and the temporal lobe were 3.39 cm/sec and 3.30 cm/sec at the inlet of the aqueduct, 3.36 cm/sec and 3.87 cm/sec at the ampulla, and

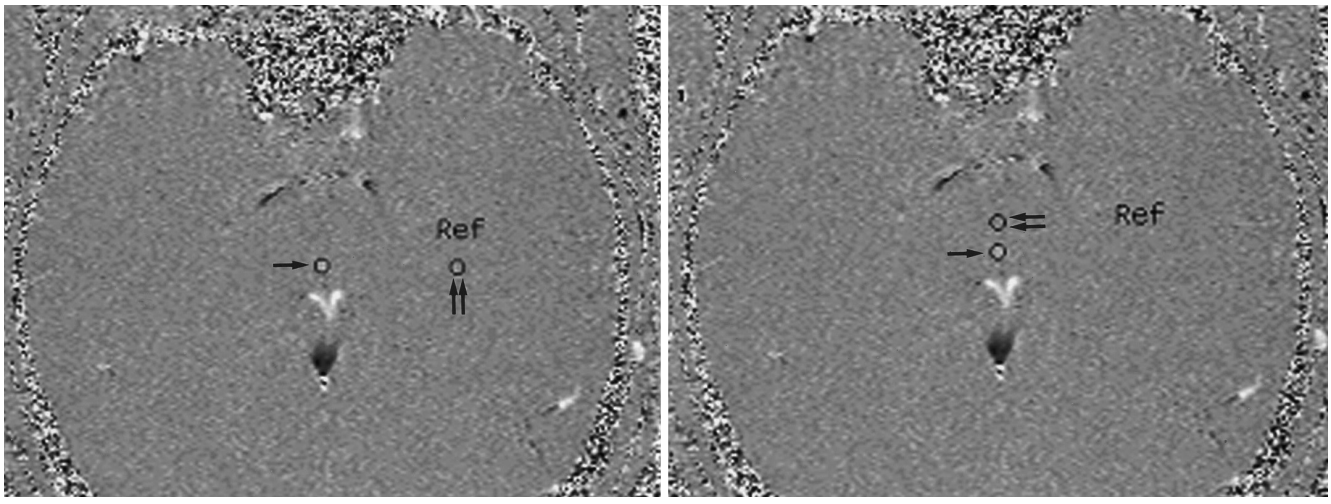

A B

Fig. 2. Selection of ROIs for the cerebral aqueduct (single arrow) and background stationary tissue (double arrows) just lateral to the aqueduct in the medial temporo-occipital gyrus (**A**) and anterior to the aqueduct in the midbrain (**B**).

4.08 cm/sec and 4.07 cm/sec at the pars posterior, respectively. However, these differences were not statistically significant (Fig. 3).

In the case of the mean flow, the values obtained with the baseline region at the anterior midbrain and the temporal lobe were 0.02 cm^3/sec and 0.02 cm^3/sec at the inlet of the aqueduct, 0.03 cm^3/sec and 0.02 cm^3/sec at the ampulla, and 0.02 cm^3/sec and 0.02 cm^3/sec at the pars posterior, respectively. There were no significant differences among the mean flows according to the location of the cerebral aqueduct or the baseline ROI (Table 1).

DISCUSSION

In CSF flow quantification using 2D phase-contrast MR imaging, the wide physiological range of the temporal,

Table 1. Mean Peak Systolic Velocities and Mean Flows According to the Location of the Cerebral Aqueduct and the Background Baseline Region

	Peak Systolic Velocity (cm/sec, mean ±SD*)		Mean Flow (cm^3/sec, mean ±SD*)	
Baseline Region / Locations	Midbrain	Temporal Lobe	Midbrain	Temporal Lobe
Inlet	3.39 ±1.61	3.30 ±1.69	0.02 ±0.0125	0.02 ±0.0141
Ampulla	3.65 ±1.59	3.87 ±1.51	0.03 ±0.0132	0.02 ±0.0151
Pars posterior	4.08 ±1.99	4.07 ±2.02	0.02 ±0.0125	0.02 ±0.0100

Note.—*: standard deviation

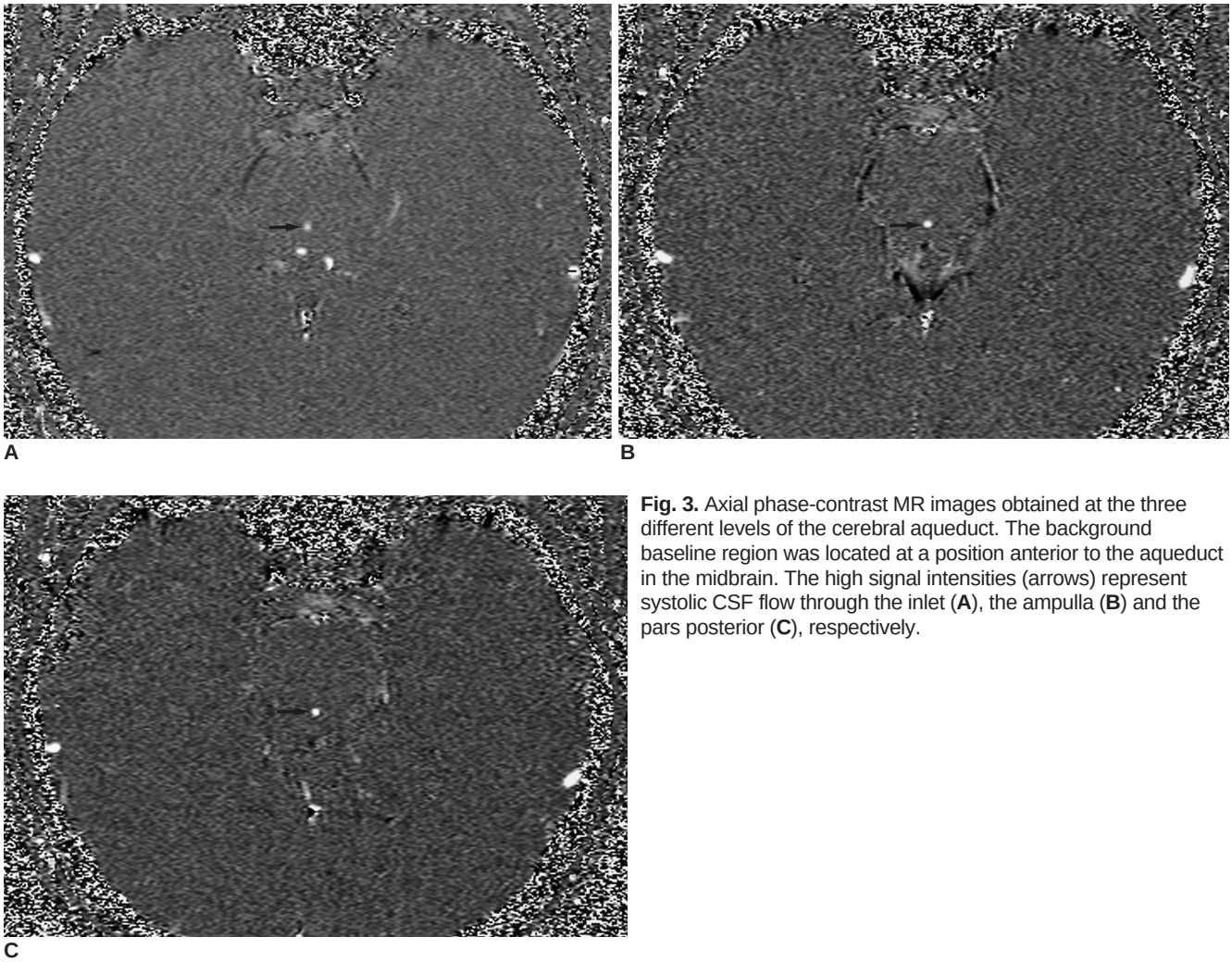

Fig. 3. Axial phase-contrast MR images obtained at the three different levels of the cerebral aqueduct. The background baseline region was located at a position anterior to the aqueduct in the midbrain. The high signal intensities (arrows) represent systolic CSF flow through the inlet (**A**), the ampulla (**B**) and the pars posterior (**C**), respectively.

velocity and flow parameters is striking (4, 5, 16). This normally wide variation is mainly related to the size and anatomy of the CSF spaces, the size of the blood vessels, the systolic and diastolic arterial blood pressure, heart rate, jugular venous flow, compliance of surrounding brain tissue, and respiration (5, 6, 8, 22, 23). The systolic temporal parameters are less variable than the diastolic parameters, because the diastole is mainly influenced by variations in the R-R interval (5, 7). Despite the use of high-resolution imaging units, there remains a considerable inaccuracy in the velocity data caused by the nonlinearity of the gradients, eddy currents, partial volume effects and the placement of the ROI (4, 18). Eddy currents cause distortion of the gradient profile, thus reducing the fidelity of the resulting encoded image. The estimated error resulting from these factors is reported to be approximately 10 to 15% (16). In the case of very narrow aqueducts, this error may be even higher, because noise and poor contrast make the placement of the ROI difficult.

In this study, we investigated two of the potential sources of the wide physiological range of the results of the CSF flow quantification. One was associated with measuring the anatomical location of the cerebral aqueduct, and the other with the selection of the baseline region used to correct the possible systematic errors caused by imperfect suppression of the eddy current.

Regardless of the location of the baseline region, a small increase in the peak systolic velocities of the CSF was observed in the measurements taken from the top to the bottom of the cerebral aqueduct, but little difference was found among the mean flows in any of the subjects. In previous studies, the CSF flow dynamics were studied at different locations of the cerebral aqueduct (18, 20, 21). Some authors reported that the most accurate measurements of the CSF flow were obtained at the narrowest point of the aqueduct, namely the inferior colliculi level (18). In another report, the aqueductal measurement was made at its junction with the fourth ventricle, in order to minimize the angle of the flow with respect to the flow-encoding axis and to minimize the partial volume effect (21). As mentioned above, anatomically, the cerebral aqueduct is divided into three parts, namely the pars anterior, ampulla and pars posterior, which are separated by two natural constrictions of the aqueductal lumen. The pars posterior has the narrowest lumen of the cerebral aqueduct (19). Contrary to our hypothesis, however, the results of our study didn't show any statistical difference according to the anatomical level of the cerebral aqueduct in the healthy volunteers. This may be because the variation in the cross-sectional area is too trivial to cause statistically significant differences in the CSF flow dynamics, or because of variations in the compliance of the cerebral aqueduct between the different levels.

In terms of the selection of which baseline region to use, we hypothesized that the anterior midbrain would be more optimal than the temporal lobe lateral to the cerebral aqueduct, because the null background offset due to eddy currents varies less along the phase-encoding direction than along the frequency-encoding direction (18). However, the statistical analysis revealed no significant difference between the two locations. This result suggests that the eddy current along the frequency or phase-encoding direction may not have a significant influence on the CSF flow quantification in 2D phase-contrast MR imaging.

Another aspect of this study which is worth mentioning is that we obtained the reference data for the CSF peak velocity and mean flow through the cerebral aqueduct in young healthy volunteers. The CSF peak systolic velocities and mean flows measured in our investigation were in good accordance with the results of previous studies, which showed that the ranges of peak systolic velocity and mean flow were -2.0 – -11.5 cm/sec and -0.06 to -0.34 cm^3/sec, respectively (16, 18).

The CSF flow quantification in 2D phase-contrast MRI used in this study had a technical limitation related to the placement of the ROI. Because the cerebral aqueduct is very small, ranging from 2 –3 mm in diameter (2), adjusting the ROI precisely to the flow pixels might be difficult, and this could result in the necessity to perform partial volume averaging of static brain tissue. Partial volume errors can result in falsely low peak systolic velocities and falsely high mean flows, which are aggravated when using a small ROI. Perpendicular imaging plane positioning and adjusting the ROI to the size of the cerebral aqueduct minimized this potential source of error. In addition, patients with aqueductal stenosis usually show widening of the beginning of the aqueduct and a relatively spared end. Therefore, the standardized use of the ampulla for CSF flow quantification, the widest area of the cerebral aqueduct, would help to further diminish this kind of error, and to obtain a better understanding of the normal and pathologic changes in the CSF flow dynamics and the clinical application of this information. To minimize the partial volume effect in the measurements made with the ROI, the mid-portion of the cerebral aqueduct would be the optimal position to use in order to study the CSF flow dynamics in both the normal and patient groups.

Previous experimental studies revealed the accuracy of MR phase contrast velocity measurements for steady and unsteady flows (25, 26) using a simplified straight tube. Actually, CSF flow through the cerebral aqueduct is not

free from secondary velocities and other complicating effects. Validation of the MR phase contrast technique for in vivo measurement may well occur in the near future.

In conclusion, we obtained a reference data set of CSF peak velocities and mean flows through the cerebral aqueduct in young healthy volunteers. Although the peak systolic velocity and mean flow of the CSF differed somewhat according to the level of the cerebral aqueduct at which the measurement was taken, the difference was not statistically significant.

Acknowledgements

The authors wish to thank Bonnie Hami, MA, Department of Radiology, University Hospitals Health System, Cleveland, Ohio, for her editorial assistance in preparing the manuscript.

References

1. Ohara S, Negai H, Matsumoto T, Banno T. MR imaging of CSF pulsatory flow and its relation to intracranial pressure. *J Neurosurg* 1988;69:675-682
2. Quencer RM, Post MJ, Hinks RS. Cine MR in the evaluation of normal and abnormal CSF flow: intracranial and intraspinal studies. *Neuroradiology* 1990;32:371-391
3. Nitz WR, Bradley WG Jr, Wantanabe AS, et al. Flow dynamics of cerebrospinal fluid: assessment with phase-contrast velocity MR imaging performed with retrospective cardiac gating. *Radiology* 1992;183:395-405
4. Henry-Feugeas MC, Idy-Peretti I, Blanchet B, Hassine D, Zannoli G, Schouman-Claeys E. Temporal and spatial assessment of normal cerebrospinal fluid dynamics with MR imaging. *Magn Reson Imaging* 1993;11:1107-1118
5. Bhadelia RA, Bogdan AR, Wolpaert SM. Analysis of cerebrospinal fluid flow waveforms with gated phase-contrast MR velocity measurements. *AJNR Am J Neuroradiol* 1995;16: 389-400
6. Bhadelia RA, Bogdan AR, Kaplan RF, et al. Cerebrospinal fluid pulsation amplitude and its quantitative relationship to cerebral blood flow pulsations: a phase-contrast MR flow imaging study. *Neuroradiology* 1997;39:258-264
7. Levy LM, Di Chiro G. MR phase imaging and cerebrospinal fluid flow in the head and spine. *Neuroradiology* 1990;32:399-406
8. Naidich TP, Altman NR, Conzalez-Arias SM. Phase contrast cine magnetic resonance imaging: normal cerebrospinal fluid oscillation and applications to hydrocephalus. *Neurosurg Clin N Am* 1993;4:677-705
9. Henry-Feugeas MC, Idy-Peretti I, Baledent O, et al. Cerebrospinal fluid flow waveforms: MR analysis in chronic adult hydrocephalus. *Invest Radiol* 2001;36:146-154
10. Luetmer PH, Huston J, Friedman JA, et al. Measurement of cerebrospinal fluid flow at the cerebral aqueduct by use of phase-contrast magnetic resonance imaging: technique validation and utility in diagnosing idiopathic normal pressure hydrocephalus. *Neurosurgery* 2002;50:534-543
11. Mascalchi M, Arnetoli G, Inzitari D, et al. Cine-MR imaging of aqueductal CSF flow in normal pressure hydrocephalus syndrome before and after CSF shunt. *Acta Radiol* 1993;34: 586-592
12. Schroeder HWS, Schweim C, Schweim H, Gaab MR. Analysis of aqueductal cerebrospinal fluid flow after endoscopic aqueductoplasty by using cine phase-contrast magnetic resonance imaging. *J Neurosurg* 2000;93:237-244
13. Bradely WG Jr, Scalzo D, Queralt J, et al. Normal-pressure hydrocephalus: evaluation with cerebrospinal fluid flow measurements at MR imaging. *Radiology* 1996;198:523-529
14. Gideon P, Stahlberg F, Thomsen C, et al. Cerebrospinal fluid flow and production in patients with normal pressure hydrocephalus studied by MRI. *Neuroradiology* 1994;36:210-215
15. Kadowaki C, Hara M, Numoto M, et al. Cine magnetic resonance imaging of aqueductal stenosis. *Childs Nerv Syst* 1995;11:107-111
16. Kolbitsch C, Schocke M, Lorenz IH, Kremser C, Zschiegner F, Pfeiffer KP, et al. Phase-contrast MRI measurement of systolic cerebrospinal fluid peak velocity (CSFV(peak)) in the aqueduct of Sylvius: a noninvasive tool for measurement of cerebral capacity. *Anesthesiology* 1999;90:1546-1550
17. Gideon P, Thomsen C, Stahlberg F, Henriksen O. Cerebrospinal fluid production and dynamics in normal aging: a MRI phase-mapping study. *Acta Neurol Scand* 1994;89:362-366
18. Barkhof F, Kouwenhoven M, Scheltens P, Sprenger M, Algra P, Valk J. Phase-contrast cine MR imaging of normal aqueductal CSF flow. *Acta Radiol* 1994;35:123-130
19. Barkhof F, Kouwenhoven M, Scheltens P, Sprenger M, Algra P, Valk J. Phase-contrast cine MR imaging of normal aqueductal CSF flow. *Acta Radiol* 1994;35:123-130
20. Baledent O, Henry-Feugeas MC, Idy-Peretti I. Cerebrospinal fluid dynamics and relation with blood flow. A magnetic resonance study with semiautomated cerebrospinal fluid segmentation. *Invest Radiol* 2001;36:368-377
21. Enzmann DR, Pelc NJ. Normal flow patterns of intracranial and spinal cerebrospinal fluid defined with phase-contrast cine MR imaging. *Radiology* 1991;178:467-474
22. Alperin N, Vikingstad EM, Gomez-Anson B, et al. Hemodynamically independent analysis of cerebrospinal fluid and brain motion observed with dynamic phase contrast MRI. *Magn Reson Med* 1996;35:741-754
23. Schroth G, Klose U. Cerebrospinal fluid flow. II. Physiology of respiration-related pulsations. *Neuroradiology* 1992;35:10-15
24. Nathan BR. *Cerebrospinal fluid and intracranial pressure*. In: Goetz CG, Pappert EJ, eds. *Textbook of Clinical Neurology*. 1st ed. St. Louis: W. B. Saunders 1999:475-486
25. Frayne R, Steinman DA, Ethier R, Rutt BK. Accuracy of MR phase contrast velocity measurements for unsteady flow. *J Magn Reson Imaging* 1995;4:428-431
26. Ku DN, Biancheri CL, Pettigrew RI, Peifer JW, Markou CP, Engles H, Evaluation of magnetic resonance velocimetry for steady flow. *ASME J Biomech Eng* 1990;112:464-472